Continuously tunable femtosecond delay-line based on liquid crystal cells

Aurélie Jullien, Umberto Bortolozzo, Stéphanie Grabielle, Jean-Pierre Huignard, Nicolas Forget, Stefania Residori

Continuously tunable femtosecond delay-line based on liquid crystal cells

Aurélie Jullien,[1,*] **Umberto Bortolozzo,**[1] **Stéphanie Grabielle,**[2] **Jean-Pierre Huignard,**[3] **Nicolas Forget,**[2] **and Stefania Residori**[1]

[1]*Institut Non Linéaire de Nice, Université de Nice Sophia-Antipolis, CNRS UMR 7335, 1361 route des Lucioles, 06560 Valbonne, France*
[2]*Fastlite, Les collines de Sophia, 1900 route des cretes, 06560 Valbonne, France*
[3] *Jphopto, 20 Rue Campo Formio, 75013 Paris, France*
[*]*Aurelie.Jullien@inln.cnrs.fr*

Abstract: We introduce a new device for group and phase delay steering of femtosecond pulse trains that makes use of cascaded, electrically driven, nematic liquid-crystal cells. Based on this approach we demonstrate a continuously tunable optical delay line. The simple collinear implementation with no moving parts enables to shape the achievable temporal range with sub-femtosecond accuracy. By appropriately choosing the bias voltages applied to the cascaded cells, the imparted group delay can be made either positive or negative and precisely adjusted. Moreover, independent control of the group delay and the phase of femtosecond pulses is demonstrated.

OCIS codes: (140.7090) Ultrafast lasers; (320.5540) Pulse shaping; (230.3720) Liquid-crystal devices.

References and links

1. A. M. Weiner, "Ultrafast optical pulse shaping: A tutorial review," Opt. Comm. **184,** 3669-3692 (2011).
2. F. Krausz and M. Ivanov, "Attosecond physics," Rev. Mod. Phys. **81**, 163-234 (2009).
3. I. A. Walmsley and C. Dorrer, "Characterization of ultrashort electromagnetic pulses," Adv. of Opt. and Phot. **1,** 308-437 (2009).
4. A. Börzsönyia, A.P. Kovacs, M. Gorbe and K. Osvay, "Advances and limitations of phase dispersion measurement by spectrally and spatially resolved interferometry," Opt. Comm. **281,** 3051-3061 (2008).
5. P. Tian, D. Keusters, Y. Suzaki and W. S. Warren, "Femtosecond Phase-Coherent Two-Dimensional Spectroscopy," Science **300,** 1553 (2003).
6. T. Brixner, I. V. Stiopkin and G. R. Fleming, "Tunable two-dimensional femtosecond spectroscopy," Opt. Lett. **29,** 884-886 (2004).
7. J. Rehault, M. Maiuri, A. Oriana and G. Cerullo "Two-dimensionnal electronic spectroscopy with birefringent wedges," Rev. of Sci. Inst. **85,** 123107 (2014).
8. A. Kolomenskii, J. Strohaber, N. Kaya, G. Kaya, A. V. Sokolov and H. A. Schuessler "White-light generation control with crossing beams of femtosecond laser pulses," Opt. Express **24,** 282-293 (2016).
9. S. Zhou, F. W. Wise and D. G. Ouzounov, "Divided-pulse amplification of ultrashort pulses," Opt. Lett. **32,** 871-873 (2007).
10. M. Hanna, F. Guichard, Y. Zaouter, D. N Papadopoulos, F. Druon and P. Georges, "Coherent combination of ultrafast fiber amplifiers," Journ. of Phys. B **49,** 062004 (2016).
11. D. Brida, C. Manzoni and G. Cerullo, "Phase-locked pulses for two-dimensional spectroscopy by a birefringent delay line," Opt. Lett. **37,** 3027-3029 (2012).
12. H. Jacqmin, A. Jullien, B. Mercier, M. Hanna, F. Druon, D. Papalopoulos and R. Lopez-Martens, "Passive coherent combining of CEP-stable few-cycle pulses from a temporally divided hollow fiber compressor," Opt. Lett. **40,** 709-711 (2015).
13. H. Jacqmin, A. Jullien, B. Mercier and R. Lopez-Martens, "Temporal pulse division in hollow fiber compressors," J. Opt. Soc. Am. B, **32,** , 1901-1909 (2015).
14. D.-K. Yang and S.-T. Wu, *Fundamentals of Liquid Crystal Devices* Wiley (2012).

#263766 Received 21 Apr 2016; revised 7 Jun 2016; accepted 10 Jun 2016; published 17 Jun 2016

15. I.-C. Khoo, Liquid crystals, *Physical Properties and Nonlinear Optical Phenomena* Wiley (1995).
16. S.-T. Wu, U. Efron and L. D. Hess, "Birefringence measurements of liquid crystals," App. Opt. **23,** 3911-3915 (1984).
17. U. Bortolozzo, S. Residori and J.-P. Huignard, "Transmissive liquid crystal light-valve for near-infrared applications," App.Opt. **52,** E73-E77 (2013).
18. S. Residori, U. Bortolozzo and J.-P. Huignard, "Slow and Fast Light in Liquid Crystal Light Valves," Phys. Rev. Lett. **100,** 203603 (2008).
19. T. Kuki, H. Fujikake, T. Nomoto and Y. Utsumi, "Design of a Microwave Variable Delay Line Using Liquid Crystal, and a Study of Its Insertion Loss," Electron. Comm. in Japan **85,** 90-96 (2002).
20. D. Dolfi, M. Labeyrie, P. Joffre and J.-P. Huignard, "Liquid Crystal microwave phase shifter," Electron. Lett. **29,** 926-928 (1993).
21. C.-S. Yang, T.-T. Tang, P.-H. Chen, R.-P. Pan, P. Yu and C.-L. Pan, "Voltage-controlled liquid-crystal terahertz phase shifter with indium-tin-oxide nanowhiskers as transparent electrodes," Opt. Lett. **39,** 2511-2513 (2014).
22. C.-Y. Chen, C.-F. Hsieh, Y.-F. Lin, R.-P. Pan and C.-L. Pan, "Magnetically tunable room-temperature 2 pi liquid crystal terahertz phase shifter," Opt. Exp. **12,** 2625-2630 (2004).
23. N. Sanner, N. Huot, E. Audouard, C. Larat, J.-P. Huignard and B. Loiseaux, "Programmable focal spot shaping of amplified femtosecond laser pulses," Opt. Lett. **30,** 1479-1481 (2005).
24. L. Cattaneo, M. Savoini, I. Muševič, A. Kimel and T. Rasing, "Ultrafast all-optical response of a nematic liquid crystal," Opt. Exp. **23,** 14010-14017 (2015).
25. L. Song, S.E Fu, Y. Liu, J. Zhou, V. G. Chigrinov and I. C. Khoo, "Direct femtosecond pulse compression with miniature-sized Bragg cholesteric liquid crystal," Opt. Lett. **38,** 5040-5042 (2013).
26. J. Li, C.-H. Wen, S. Gauza, R. Lu and S.-T. Wu, ''Refractive Indices of Liquid Crystals for Display Applications," J. Display Techno. **1,** 51-61 (2005).
27. I. C. Khoo, "Nonlinear optics, active plasmonics and metamaterials with liquid crystals," Progress in Quantum Electronics **38,** 77-117 (2014).
28. R. Dabrowski, P. Kula and J. Herman, "High Birefringence Liquid Crystals," Crystals **3,** 44-4823 (2013).
29. L. Lepetit, G. Chériaux and M. Joffre , "Linear techniques of phase measurement by femtosecond spectral interferometry for applications in spectroscopy," J. Opt. Soc. Am. B **12,** 2467–2474 (1995).
30. S.-T. Wu and C.-S. Wu, "High speed liquid crystal modulators using transient nematic effect," Journ. of App. Phys. **65,** 527-532 (1989).
31. M. Görbe, K. Osvay, C. Grebing and Günter Steinmeyer, "Isochronic carrier-envelope phase-shift compensator," Opt. Lett. **33,** 2704-2706 (2008).
32. O. Gobert, G. Mennerat, C. Cornaggia, D. Lupinski, M. Perdrix, D. Guillaumet, F. Lepetit, T. Oksenhendler and M. Comte, "Electro-optic prism-pair setup for efficient high bandwidth isochronous CEP phase shift or group delay generation," Opt. Comm. **366,** 45-49 (2016).

1. Introduction

Ultrafast optical waveforms propagating in any dispersive medium experience different group and phase velocities. Controlling these quantities is the basis of temporal manipulation and shaping of ultrafast pulses, while stabilizing the slippage between them (carrier-to-envelope phase, CEP) has paved the way to attosecond physics [1, 2]. Group delay manipulation, among other pulse shaping objectives, provides tools for temporal division of femtosecond pulses. Devices for temporal division are widely employed for measurement and characterization of ultrashort pulses [3], self-referenced spectral interferometry [4], ultrafast spectroscopy [5, 6, 7], nonlinear optics [8] and temporal multiplexing [9, 10]. For most of these applications, accurate tunability and sub-fs resolution of the introduced delay are required. As a complement to mechanical delay lines, collinear setups based on birefringent elements ensure simplicity, compactness and robustness. However, the achievable delays are discrete and characterized by little tunability. A couple of elegant solutions mixing collinearity and continuous tunability have been recently proposed : birefringent wedges for electronic spectroscopy [11] and tilting birefringent plates with out-of-axis orientation for coherent combining of ultrashort pulses [12, 13]. Both schemes are based on crystallographic material and require mechanical action on it, which could result in a certain numbers of drawbacks due to the moving parts.

In this paper, we propose to exploit the large and electrically-controllable birefringence of nematic liquid crystals for precise control of the group and phase delays of femtosecond pulses. To that purpose, liquid crystals intrinsically present very interesting optical features : a much

#263766 Received 21 Apr 2016; revised 7 Jun 2016; accepted 10 Jun 2016; published 17 Jun 2016

higher birefringence than crystals, together with the ability to change their optical properties through molecular reorientation in response to a low voltage or weak magnetic field. Extensively studied for light manipulation and control [14, 15], liquid-crystals have been, for instance, demonstrated as tunable phase-shifter for optical laser frequencies [16], nonlinear optical Kerr elements in light-valve configuration [17, 18], tunable delay line or phase-shifter in the microwave band [19, 20], or efficient phase-shifters for THz radiation, with either voltage [21] or magnetic control [22]. However, even though liquid crystals are transparent and highly birefringent over a broad spectral range [15], application to the manipulation of ultrashort pulses has been quite occasional so far. Apart from spectral or spatial shaping by spatial-light-modulators in the Fourier plane [1, 23], only a very few studies report on the use of liquid-crystals for direct manipulation of ultrafast pulses, either via a coherently excited nonlinear response in nematics [24] or by exploiting the Bragg resonance in a cholesteric cell [25].

Here, we demonstrate an innovative and efficient device to control the group and phase delay of femtosecond pulses, which is realized by appropriately addressing one or two electrically-driven nematic liquid-crystal cells. Based on this approach, we first focus on the group delay tuning with a single nematic cell and demonstrate a simple, collinear, continuously tunable optical delay line suitable for ultrafast pulse trains. The tested devices afford various group delay ranges, from $\sim$10fs to $\sim$100fs, with an applied voltage between 0V and 10V. The response time evolves between second to millisecond time-scale. Electrically-controlled temporal resolution can be chosen between 2.3 fs and $<$0.1fs. Then, two cascaded liquid crystal cells are shown to provide temporal division with a delay tunable between -50fs and +50fs, and sub-fs precision. By appropriately choosing the couple of bias voltages applied to the cascaded cells, the introduced group delay can be made either positive or negative and finely adjusted around the chosen value. Finally, we highlight an additional possibility. Adequate electrical control of two cells with different thicknesses is shown to afford independent tuning of the phase and group delays. Altogether, these results demonstrate that nematic liquid-crystals cells enable the high-precision manipulation of optical pulses in the femtosecond regime. The setup is simple and offers many advantageous features, such as compactness, continuous tunability, collinearity and no moving parts.

2. Femtosecond continuously tunable delay line with a single liquid crystal cell

We first implement temporal division and group delay control of femtosecond pulses by using a single liquid-crystal cell. The tunable delay line is realized by using as the birefringent medium the nematic liquid crystal (LC) mixture E7, inserted in between two 0.7mm-thick fused-silica substrates. Both of them include a conductive layer of ITO (Indium-tin oxyde) for electrical control of the molecular director. A thin film of polyvinyl alcohol (PVA) is spin-coated on the ITO layer with subsequent rubbing to favor initial alignment of the molecules in a plane parallel to the substrate (splay geometry). Four samples with different thickness ranging from 25 μm to 130 μm were prepared. The experiment is set up as shown in Fig. 1(a). The laser system is a Femtofiber PRO IRS (Toptica Photonics) oscillator delivering 40 fs pulses, at 1570 nm, with 200 mW average power. The repetition rate is 80 MHz. The pulses are frequency-doubled in a 0.25 mm BBO crystal to produce about 30 fs pulses, with a spectrum centered at 770 nm. A half-waveplate and a polarizer set the linear polarization direction to 45° with respect to the nematic director of the LC cell, so that two sub-pulses, respectively P and S polarized, propagate through the LC cell. An analyzer, a broadband thin film polarizer parallel to the first one, projects the two cross-polarized sub-pulses onto the same polarization direction. They finally interfere in a spectrometer (Avantes). If the two sub-pulses propagate with different group delay, the interference spectrum presents fringes with a period inversely proportional to the relative delay.

#263766 Received 21 Apr 2016; revised 7 Jun 2016; accepted 10 Jun 2016; published 17 Jun 2016

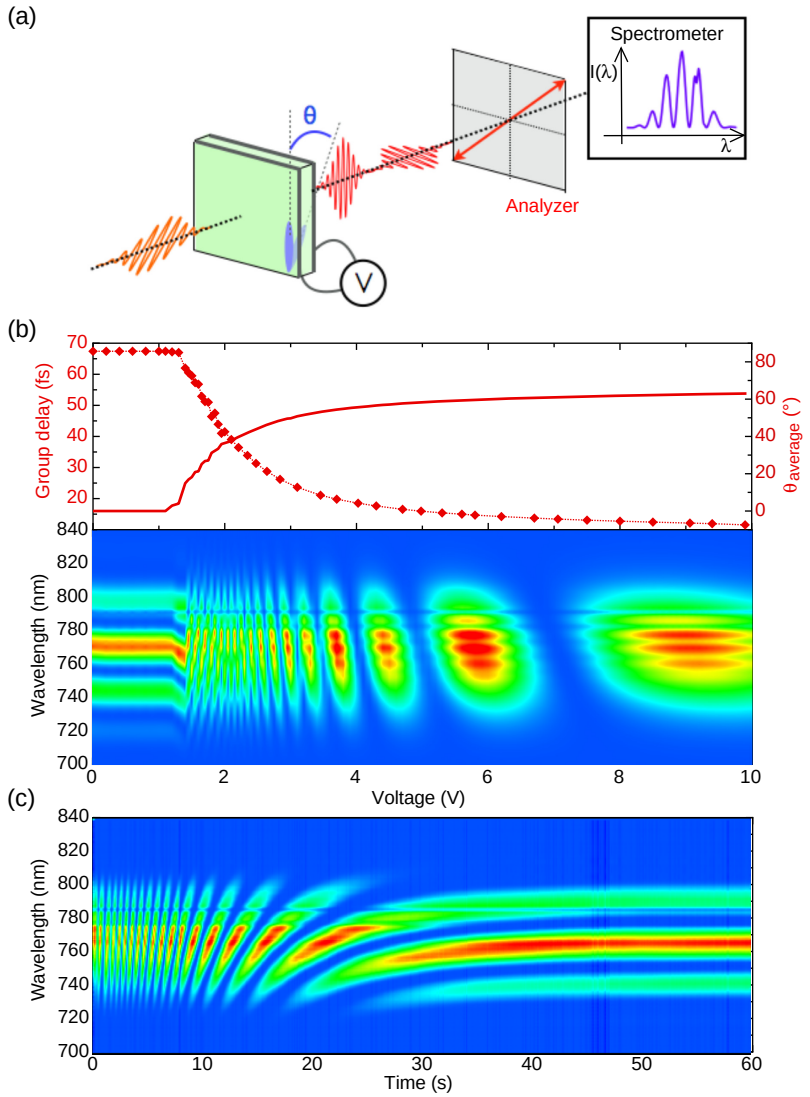

Fig. 1. (a) Principle of the experiment. Green : LC cell, blue : initial molecular orientation. (b) (colormap) Analyzed interference spectrum measured as a function of the voltage, for the 88 μm - thick LC cell. The upper graph shows the retrieved group delay (points) and corresponding tilt angle θ (solid line) averaged over the cell thickness. (c) Analyzed interference spectrum recorded regularly (2 ms) as a function of time, for the 88 μm - thick LC cell. The bias voltage of 10V is shut down at $t = 0$.

#263766 Received 21 Apr 2016; revised 7 Jun 2016; accepted 10 Jun 2016; published 17 Jun 2016

Phase and group delays acquired in the LC mixture for each polarization directions are respectively defined as :

$$\tau_{(\phi)o,e} = n_{o,e}\frac{L}{c} \tag{1}$$

$$\tau_{(g)o,e} = n_{(g)o,e}\frac{L}{c} \quad \text{with} \quad n_{(g)o,e} = n_{o,e} + \omega_0 \frac{dn_{o,e}}{d\omega} \tag{2}$$

n_o (resp. n_e) is the ordinary (resp. extraordinary) refractive index of the LC mixture, $n_{(g)o}$ (resp. $n_{(g)e}$) is the ordinary (resp. extraordinary) group index, L is the LC thickness and ω_0 the central laser frequency. In the following, group index, group delay and group delay dispersion (GDD) are calculated for $\lambda_0 = 770nm$.

The LC cells, at normal incidence, were first characterized with no voltage applied. The orientation of the nematic director is then determined by the anchoring conditions. The S-polarized pulse propagates through a purely extraordinary medium. The refractive index difference with the P-polarized ordinary wave, which is related to the birefringence of the LC mixture, is maximum and can be expressed as $\Delta n_{o-e} = n_e - n_o$. For nematic E7, in the considered spectral range, the group index difference $\Delta n_{(g)o-e}$ is 0.23 [26]. The two sub-pulses consequently emerge out of the cell with a temporal spacing proportional to the LC thickness. Simple Fourier Transform of the interference spectrum enables to recover the introduced group delay and thus to deduce the sample thickness. Cells $LC_{1,2,3}$ induce an initial group delay of 104 ± 0.2 fs, 67 ± 0.2 fs and 41 ± 0.2 fs, respectively. Uncertainty is here related to the Fourier transformation. The delay is also likely to vary by ± 1 fs on a day-to-day basis because of alignment or temperature changes. Respective thicknesses are $136 \pm 2\,\mu$m, $88 \pm 2\,\mu$m and $55 \pm 1\,\mu$m, as summarized in Table 1. A thinner cell, LC_4, leading to a delay smaller than the pulse width, was calibrated with respect to the other samples : Fourier transform of the interference spectrum produced by two successive cells with parallel orientation provides the additional group delay. LC_4 is found to be $26 \pm 1\,\mu$m-thick.

GDD introduced by E7 is $\phi_o^{(2)}$ = 120 fs^2/mm and $\phi_e^{(2)}$ = 320 fs^2/mm. Table 1 presents the total GDD for each cell, mainly originating from the substrates. Whatever the cell thickness, the transmission is 75%, limited by Fresnel losses on the uncoated substrates and absorption in the ITO layers. AR-coating and thinner ITO would raise this value.

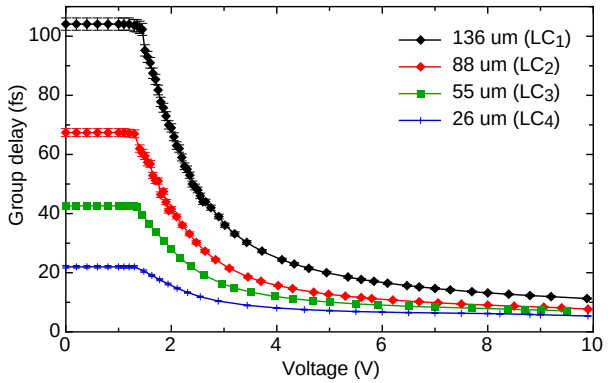

Fig. 2. Measured group delay as a function of the applied voltage, according to the liquid crystal cell thickness.

When an external electric field is applied, its interaction with the LC induces molecular reorientation [14]. As E7 presents a positive dielectric anisotropy, the molecules tend to reorient

#263766 Received 21 Apr 2016; revised 7 Jun 2016; accepted 10 Jun 2016; published 17 Jun 2016

Table 1. **Liquid crystal cells thickness, GDD ($\lambda_0 = 770nm$) in both polarization directions and properties as a tunable delay line for several bias voltages. δ_t is the temporal tunability and τ is the response time.**

		LC_1	LC_2	LC_3	LC_4
Thickness (μm)		136	88	55	26
	$\phi_o^{(2)}(fs^2)$	69	64	60	56
	$\phi_e^{(2)}(fs^2)$	95	81	71	61
2V	$\delta_t(fs/50mV)$	2.3	1.3	0.75	0.35
	$\tau(s)$	20	10	5	2
4V	$\delta_t(fs/100mV)$	0.7	0.4	0.25	0.1
	$\tau(s)$	3	1	0.7	0.1
6V	$\delta_t(fs/100mV)$	0.3	0.2	0.07	0.03
	$\tau(s)$	0.1	0.01	0.001	0.001
8V	$\delta_t(fs/100mV)$	0.1	0.07	0.04	0.03
	$\tau(s)$	0.001	0.001	0.001	0.001

along the applied electric field direction [27, 28]. A waveform generator produces a sinusoidal AC voltage (frequency 1 kHz) with an amplitude between 0V and 10V. The interference spectrum is registered as the voltage regularly increases (step : 50 mV between 1.3V and 3V, 100 mV otherwise) for each LC cell. The integration time is 1 ms and the spectrum is monitored until stability is reached. The resolution of the spectrometer is 0.3 nm, well below the narrowest fringes spacing (19 nm for a relative group delay of 100 fs). For a given bias voltage in static conditions, the stability of the interference pattern is found to lie within the spectrometer resolution. The resulting spectra are plotted as a 2D map, as shown in Fig. 1(b) for LC_2 (88 μm thick). The initial interference spectrum remains constant up to the Freedericksz transition voltage (1.2 V for E7), above which the molecules start to reorient. In the current implementation, the extraordinary index is then progressively changed according to the following law :

$$n_e(\theta) = \frac{n_o n_e}{\sqrt{cos^2\theta\ n_o^2 + sin^2\theta\ n_e^2}} \tag{3}$$

with θ the local angle formed between the nematic director and the original alignment axis. Note that θ depends on the voltage and is not uniform across the LC thickness, as reorientation occurs mostly in the middle of the cell, while closer to the substrates the anchoring conditions dominate [14]. Anyway, the average tilt angle increases with the voltage, therefore the average extraordinary index decreases as the voltage increases, inducing narrowing of the temporal spacing between the pulses and significant changes of the interference pattern. Important reorientation between 2V and 4V is followed by a saturated behavior with progressive constructive and destructive interferences. The spectrogram is analyzed with Fourier Transform Spectral Interferometry methods (FSTI, [29]) and enables to recover the introduced group delay as a function of the voltage, as shown in the upper graph of Fig. 1(b). The average refractive index, and thus the average value of θ, according to the applied voltage can be deduced from the experimental group delay. Measured reorientation as a function of the field, plotted in Fig. 1(b),

#263766 Received 21 Apr 2016; revised 7 Jun 2016; accepted 10 Jun 2016; published 17 Jun 2016

presents a typical trend [14].

Figure 2 summarizes the group delay dependence with the voltage, measured for the four considered LC cells. The group delay is easily tunable over several tens of femtosecond, depending on the initial delay fixed by the LC properties and thickness. At 10V, the medium is not purely ordinary in the S-polarization direction, as the molecular reorientation is less effective close to the substrates because of the strong anchoring conditions. The delay for this maximum voltage only slightly varies with the sample and is $\sim$10fs. The temporal tunability per voltage step is deduced from the spectrograms and is reported in Table 1. It depends on the cell thickness and the bias voltage, and is ranging from a few fs per 50mV to less than 0.1fs per 100mV. The highest resolution is reached for a high bias voltage. Under this condition, as 0.1 fs corresponds to a 250 mrad phase-shift ($\lambda_0 = 770nm$), the change is visible in the spectrogram as a shift of the interference pattern of a few nm, above the resolution of the spectrometer.

The optical response to the electric field is governed by collective motion of the molecules and rotational viscosity of the medium, and again depends on the cell thickness and the applied voltage. The response time indicated in Table 1 is measured for small voltage increment (50 mV or 100 mV) for different bias voltages (2V, 4V, 6V, 8V). The results are in good agreement with previous publications [30]. The optical response is rather slow for the larger tunability settings (a few seconds) but is significantly reduced at higher bias voltage, enabling kHz adjustment rate. Furthermore, the remanence of the molecules orientation can be used for faster acquisition of the full delay range of thick cells. As an illustration, Fig. 1(c) shows the analyzed spectrum regularly logged (every 2 ms over 1 minute, thanks to the spectrometer software), for LC_2, when the voltage is shut down from 10V to 0V at $t = 0$. The full delay range in this transient nematic state can be acquired in less than 1 minute with a temporal resolution of 0.1 fs per acquisition step. These properties may contribute to the eligibility of such devices to ultrafast pulse train manipulation.

Given these observations, applications such as ultrafast spectroscopy or coherent combining, which require fast and precise control of the group delay and/or phase delay, could benefit of the combination of two LC cells. A thick one would introduce a variable main delay while a thiner one would provide nearly real-time (for kHz or sub-kHz repetition rate laser systems), tunable, precise adjustment. Furthermore, we underline that thin LC cells can be adapted to phase-delay control and could advantageously complete bulk thin wedges currently used for CEP stabilization.

3. Cascaded liquid crystal cells

In this section, by cascading two LC cells, we realize a delay line where the relative group delay of the femtosecond pulses can be made either positive or negative depending on the values of the bias voltages.Such tunable delay line presents interesting prospects for temporal measurement purposes. In that case, both positive and negative delays are required (e.g. for an autocorrelation measurement) and controllable delay around the temporal overlap of the two sub-pulses is needed.

We performed this experiment by cascading two LC cells with crossed orientations and independent voltage control, as shown in Fig. 3(a). Under the action of the electric field, the two nematic directors are rotated by an angle θ_1 and θ_2, respectively. Two nearly identical cells are employed, presenting a thickness of 88 μm. The measurements reported in Fig. 1(b) enable to extrapolate the delay introduced by the cascaded crossed cells scheme. Figure 3(b) shows the calculated output group delay between the two sub-pulses as a function of the two voltages. For couples of identical voltages, the delay is nearly zero. The widest temporal range around the overlap is provided by increasing one voltage while decreasing symmetrically the second one.

Both cells are aligned close to auto-collimation. When no voltage is applied, the temporal

#263766 Received 21 Apr 2016; revised 7 Jun 2016; accepted 10 Jun 2016; published 17 Jun 2016

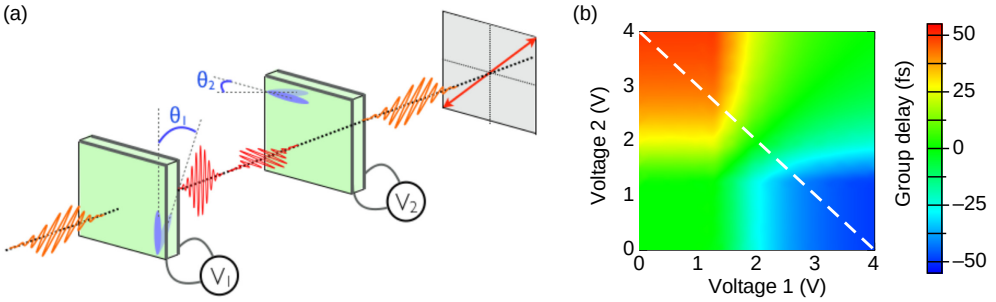

Fig. 3. (a) Tunable delay line with two cascaded LC cells with crossed orientation. (b) Extrapolated dependence of the introduced group delay as a function of the voltage applied on both cells, considering two identical birefringent media (88 μm - thick). The white line indicates the couples of bias voltages applied in the experiment.

overlap is supposed to be achieved at the output of the second cell, meaning that the two sub-pulses can be coherently added. In that case, the analyzed spectrum is identical to the input one and the transmitted energy through the analyzer is maximum. Because of a small thickness discrepancy between the two cells, a slight horizontal tilt of the second one is needed to achieve this condition. The voltage on the first cell is then increased from 0V to 4V, while the voltage on the second cell is simultaneously decreased from 4V to 0V. The increment step is 10 mV for both voltages. The interference spectra are registered after the analyzer following the procedure described in the previous section. The resulting group delay evolution issued from FTSI analysis is shown in Fig. 4.

The achievable group delay is tunable over -50fs / +50fs temporal range, with a linear dependence with the voltage between $V_1 \sim 1.5V$ and $V_1 \sim 2.5V$. The analyzed spectrum map for $1.6V < V_1 < 2.4V$ is plotted in Fig. 4(b). One can see wavelength-dependent constructive and destructive interferences, as a function of the two applied voltages. As the voltages tune the relative delay, the map is a spectrally-resolved correlation of the fields of the two sub-pulses. When the temporal overlap is reached (envelopes and carrier waves), all the spectral components are coherently added and transmitted through the analyzer. The overlap is indicated on the spectrogram ($V_1 = 2.06V$, $V_2 = 2.05V$) and the input laser spectrum is then fully recovered after the analyzer, as shown in Fig. 4(c). The spectral shift of the interference pattern between each acquisition step provides the achievable temporal resolution in this portion : 0.5 fs per acquisition step. Higher resolution can be achieved by reducing the voltage increment or by choosing other couples of voltage values, according to Fig. 3(b).

This experiment demonstrates the eligibility of the proposed setup for collinear coherent combining of femtosecond pulses. Furthermore, this crossed LC cells device is a simple, achromatic delay line suitable for autocorrelation-based temporal measurements of ultrashort pulses. GDD is here $\sim$145 fs^2 and can be reduced by using thinner substrates and combining the cells so as to remove one interface. The overall temporal range can be simply extended by using other liquid crystal material or increasing the cell thickness.

4. Independent control of the phase and group delay

To further emphasize the pulse shaping skills of the proposed device, we also demonstrate the ability to independently control the group delay or the phase of the propagating pulse. Such features are of interest for CEP-controlled ultrafast laser or OPA systems. Furthermore, changing the phase with no modification of the delay (e.g. timing) or changing the relative

#263766 Received 21 Apr 2016; revised 7 Jun 2016; accepted 10 Jun 2016; published 17 Jun 2016

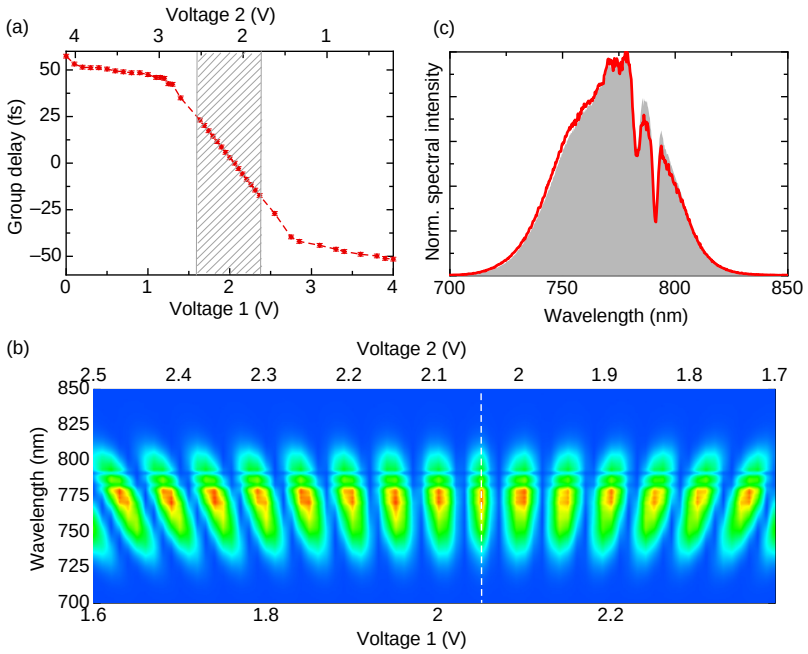

Fig. 4. (a) Group delay measured at the output of the cascaded cells as presented in Fig. 3(a), as a function of the voltages (V_1 and V_2, two x-axis graduations) applied on the two cells. The cells present nearly identical thickness (88 μm). Their initial director orientations are crossed. (b) Measured output spectrum for a narrower voltage range (hatched area in (a)). A white line indicates the temporal overlap (see text). (c) Corresponding output spectrum (red, $V_1 = 2.06V$, $V_2 = 2.05V$) compared to the initial laser spectrum (shaded).

spacing between two pulses with constant relative phase might provide an additional insight in high-resolution pump-probe experiments. So far, such capabilities have been demonstrated with bulk prism pairs : thin wedges made from carefully chosen optical material [31] and electro-optic prisms of RTP crystal [32]. Both methods require accurate sizing and angular orientation of the prisms.

The principle relies on the different evolution of the group index (resp. group delay) and the refractive index (resp. phase delay) in the LC as a function of θ, for the wave polarized in the rotation plane of the molecular director under the action of the electric field. In order to achieve independent control of the phase and group delay of this wave, two cascaded cells with separate voltage control are needed. Furthermore, the capability to produce very thin LC cells ($< 10\mu m$) eases the experimental realization.

Figure 5(a) shows the tested implementation : two cells are positioned at normal incidence with parallel orientations. They present different thicknesses : LC_1 (136 μm) is used together with a fifth cell, whose measured LC (E7) thickness is 8.2 μm . For such a cell, the maximum relative group delay introduced when no voltage is applied is 6.3 fs. In the discussed setup, the relative group delay and the relative phase between the two sub-pulses can be simply expressed as :

$$\Delta t = \frac{1}{c}[n_{(g)e}(\theta_1)L_1 + n_{(g)e}(\theta_2)L_2 - n_{(g)o}(L_1 + L_2)] \tag{4}$$

$$\Delta\phi = \frac{2\pi}{\lambda}[n_e(\theta_1)L_1 + n_e(\theta_2)L_2 - n_o(L_1 + L_2)] \tag{5}$$

#263766
Received 21 Apr 2016; revised 7 Jun 2016; accepted 10 Jun 2016; published 17 Jun 2016

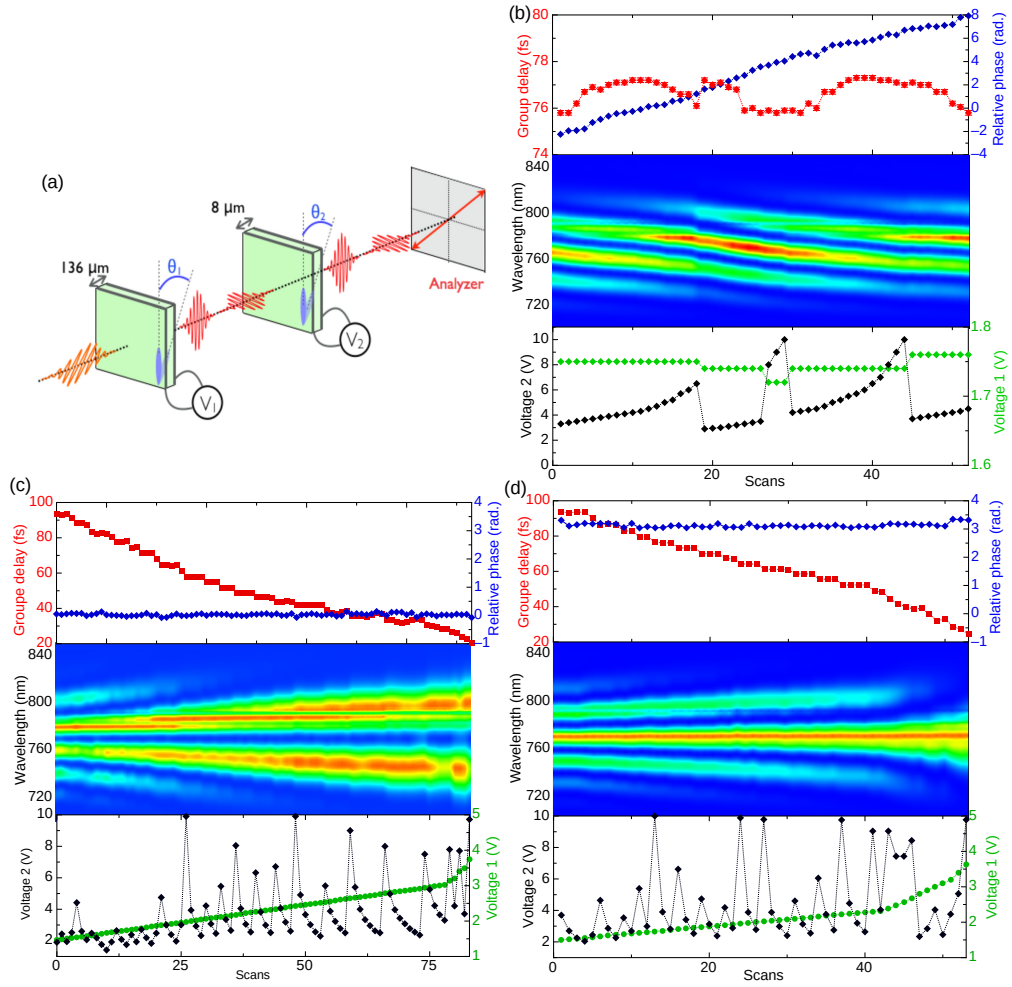

Fig. 5. (a) Cascaded LC cells with parallel orientations for independent control of the phase and group delay. Phase control (b) and group delay control for two different phase values (c,d) : measured group delay and relative phase (upper graphs) and corresponding spectra registered after the analyzer (middle graphs). The data are successfully recorded for different couples of voltage values indicated on the lower graphs.

where $L_1 = 136\mu m$, $L_2 = 8.2\mu m$, $n_{(g)e}(\theta)$ and $n_e(\theta)$ are defined according to Eq. (2) and Eq. (3). θ_1 and θ_2, the molecular orientations in each cell, are the two tunable parameters, through the applied voltages V_1 and V_2.

Given the respective cell thicknesses, the first one mainly manages the relative group delay, while full voltage excursion on the second enables to adjust the relative phase. Finally, in this setup, the ordinary wave (P-polarized) can be seen as a reference beam, as its propagation is not affected by the molecular reorientation. The extraordinary wave alone undergoes group delay and phase changes. The interference spectrum between the two waves measured after the analyzer enables to monitor and analyze those changes.

The two voltages are first tuned to change the phase continuously, while keeping constant the group delay. Measured group delay, phase and the resulting spectrogram are shown in Fig. 5(b). In this case, the voltage rise on the thin cell affords phase excursion while minor voltage varia-

#263766 Received 21 Apr 2016; revised 7 Jun 2016; accepted 10 Jun 2016; published 17 Jun 2016

tions on the thick one enables to maintain the group delay nearly constant. The required voltage increments are 100 mV for V_2 and 10 mV for V_1. As a result, the phase can be adjusted over 2.5π with a precision of 200 mrad while the group delay excursion is reduced to 1.5 fs.

Symmetrically, the group delay can be tuned while the phase is maintained to an arbitrary chosen value. This is illustrated in Fig. 5(c,d) for two different phase values. To do so, the voltage on the first cell is progressively increased (20 mV step) from 1V to 4V to initiate significant group delay changes. The second cell, whose voltage oscillates between 2V and 10V, enables to precisely adjust the phase to the desired value. 10 mV precision is then required. In both cases, the phase is constant with 70 mrad RMS noise and the group delay evolves between 90 fs and 20 fs. The temporal resolution is better than 2 fs and could be minimized by the use of a thinner second LC cell.

The proposed simple setup composed of two cascaded LC cells offers precise pulse manipulation capabilities. The alignment is straightforward. Furthermore, the device is static, requires only low-voltage electrical control and is easily scalable in its lateral dimensions.

5. Conclusion

To conclude, we have demonstrated a femtosecond, continuously tunable, optical delay-line based on one or two cascaded nematic liquid-crystal cells. The proposed setup is versatile. The introduced group delay, response time and temporal resolution are adjustable depending on the desired application. Cascaded cells enable to shape the achievable temporal range as well as the temporal accuracy. Both the phase and group delay can be controlled with such devices, independently if needed. The experimental implementation is straightforward, no mechanical action is required as low voltage control is only needed. The proposed performances can be tuned by modifying the cascaded cells architecture, the cells thickness, the material, and the voltage increment. This scheme is suited to higher pulse energy as the lateral dimensions of the liquid-crystal cell are easily scalable. Furthermore, it can be adapted to typical wavelengths of femtosecond sources, from the visible to mid-IR. The presented results disclose an innovative approach in the manipulation of femtosecond pulse trains. Near-future applications include temporal division for pulse measurement as well as carrier-to-envelope phase control of ultrafast pulses.

Acknowledgments

The work is supported by the ANR (Agence Nationale de la Recherche) under the project Labcom SOFTLITE (ANR 15-LCV1-0002-01).

#263766 Received 21 Apr 2016; revised 7 Jun 2016; accepted 10 Jun 2016; published 17 Jun 2016